Received: 9 November 2017 | Revised: 7 August 2018 | Accepted: 6 September 2018

DOI: 10.1111/avsc.12403

RESEARCH ARTICLE

Applied Vegetation Science IAVS

Remote sensing of β-diversity: Evidence from plant communities in a semi-natural system

Samuel Hoffmann[1] | Thomas M. Schmitt[1] | Alessandro Chiarucci[2] | Severin D. H. Irl[1] | Duccio Rocchini[3,4,5] | Ole R. Vetaas[6] | Mihai A. Tanase[7,8] | Stéphane Mermoz[7] | Alexandre Bouvet[7] | Carl Beierkuhnlein[1]

[1]Department of Biogeography, BayCEER, University of Bayreuth, Bayreuth, Germany

[2]Department of Biological, Geological, and Environmental Sciences, Alma Mater Studiorum, University of Bologna, Bologna, Italy

[3]Center Agriculture Food Environment, University of Trento, S. Michele all'Adige (TN), Italy

[4]Centre for Integrative Biology, University of Trento, Povo (TN), Italy

[5]Department of Biodiversity and Molecular Ecology, Fondazione Edmund Mach, Research and Innovation Centre, S. Michele all'Adige (TN), Italy

[6]Department of Geography, University of Bergen, Bergen, Norway

[7]Center for the Study of the Biosphere from Space (CESBIO), Toulouse, France

[8]Department of Geology, Geography and Environment, University of Alcala, Alcalá de Henares, Spain

Correspondence
Samuel Hoffmann, Department of Biogeography, BayCEER, University of Bayreuth, Bayreuth, Germany.
Email: samuel.hoffmann@uni-bayreuth.de

Funding information
This study was funded by the ECOPOTENTIAL project - EU Horizon 2020 research and innovation programme, grant agreement No. 641762.

Co-ordinating Editor: Hannes Feilhauer

Abstract

Question: Do remote sensing signals represent β-diversity? Does β-diversity agree with community types?

Location: UNESCO Man and the Biosphere Reserve, La Palma, Canary Islands.

Methods: We recorded perennial, vascular plant species abundances in 69 plots (10 m × 10 m) in three pre-defined community types along an elevational gradient of 2,400 m: succulent scrubland, *Pinus canariensis* forest and subalpine scrubland. The remote sensing data consists of structural variables from airborne Light Detection and Ranging (LiDAR) and multispectral variables from a time series of Sentinel-2 (S2) images. Non-metric Multidimensional Scaling was used to assess β-diversity between plots. *K*-means unsupervised clustering was applied to remote sensing variables to distinguish three community types. We subsequently quantified the explanatory power of S2 and LiDAR variables representing β-diversity via the Mantel test, variation partitioning and multivariate analysis of variance. We also investigated the sensitivity of results to grain size of remote sensing data (20, 40, 60 m).

Results: The β-diversity between the succulent and pine community is high, whereas the β-diversity between the pine and subalpine community is low. In the wet season, up to 85% of β-diversity is reflected by remote sensing variables. The S2 variables account for more explanatory power than the LiDAR variables. The explanatory power of LiDAR variables increases with grain size, whereas the explanatory power of S2 variables decreases.

Conclusion: At the lower ecotone, β-diversity agrees with the pre-defined community distinction, while at the upper ecotone the community types cannot be clearly separated by compositional dissimilarity alone. The high β-diversity between the succulent scrub and pine forest results from positive feedback switches of *P. canariensis*, being a fire-adapted, key tree species. In accordance with the spectral variation hypothesis, remote sensing signals can adequately represent β-diversity for a large extent, in a short time and at low cost. However, in-situ sampling is necessary to fully understand community composition. Nature conservation requires such interdisciplinary approaches.

KEYWORDS
β-diversity, conservation biogeography, elevation gradient, island biogeography, LiDAR, plant community, remote sensing, Sentinel, spectral variation hypothesis, time series, tree line, vegetation indices

1 | INTRODUCTION

The spatial and temporal change rates of species composition, i.e. β-diversity, have been at the heart of community ecology ever since Clements (1916). However, the community definition is still largely debated (Chiarucci, 2007; Palmer & White, 1994; Ricklefs, 2008). The controversy revolves around the coherence and integrity of ecological entities through different scales of space and time (Jax, 2006). In order to assess community patterns, concepts of β-diversity are applied that quantify the compositional dissimilarity between species assemblages (Anderson et al., 2011).

Processes responsible for observed patterns of species coexistence, usually referred to as "assembly rules", can be deterministic, stochastic, interrelated and contingent, which led Lawton (1999) to call community ecology "a mess". Vellend (2010) proposed the following overarching processes shaping β-diversity and community patterns: selection, drift, speciation and dispersal. These factors and anthropogenic activities determine β-diversity and, thus, biodiversity in general (Socolar, Gilroy, Kunin, & Edwards, 2016), on which human well-being depends (Cardinale et al., 2012). It is therefore important to study patterns of β-diversity as well as corresponding drivers.

The existence of communities implies the delineation of community types. Because natural boundary sharpness varies (Auerbach & Shmida, 1993; Wilson & Agnew, 1992), community distinction is not necessarily discrete; transition between communities can be rather continuous. This is why community limits are specifically considered as transition zones, also known as ecotones (Livingston, 1903). In early times, an ecotone was associated with a clear separation of plant physiognomy (Clements, 1905). The recent definition of ecotone by Lloyd, McQueen, and Lee (2000) is based on β-diversity and describes it as a "zone where directional change in vegetation (i.e. qualitative and quantitative species composition) is more rapid than on the other side of the zone." Although ecotones are a standard entity in landscape ecology (Wiens, Crawford, Gosz, Crawford, & Boundary, 1985), Hufkens, Scheunders, and Ceulemans (2009) point out that they do not have standardized spatial and temporal units.

In order to analyse the spatial and temporal complexity of plant communities, comprehensive field sampling and monitoring is needed, which is time-consuming and costly. Remote sensing (RS) can be a powerful tool to estimate β-diversity patterns over large extents, in a short time and at low cost (Rocchini et al., 2016). RS sensors provide data that reveal biodiversity patterns from local to global extent as well as patterns that are temporally resolved. RS sensors are used to detect changes in community composition, with changes in spectral diversity as a measure of β-diversity (Rocchini, Butini, & Chiarucci, 2005). This application rests on the spectral variation hypothesis (SVH) explaining the relationship between environmental heterogeneity, species diversity and spectral information (Palmer, Earls, Hoagland, White, & Wohlgemuth, 2002). Environmental heterogeneity increases habitat heterogeneity and, thus, species diversity (i.e. habitat heterogeneity hypotheses; Simpson, 1949). Environmental heterogeneity also increases spectral heterogeneity. Therefore, spectral variation is associated with α- and β-diversity (Palmer et al., 2002; Rocchini, Chiarucci, & Loiselle, 2004). However, the SVH does not apply to all ecosystems and depends on the extent of RS and in-situ data as well as the spatial, temporal and spectral resolution of RS data (Schmidtlein & Fassnacht, 2017).

This study relates to the SVH, because we investigate to what degree RS signals of species assemblages can explain β-diversity, i.e. the compositional dissimilarity between species assemblages. As a case study, we sampled the semi-natural plant communities along a continuous elevational gradient on La Palma, Canary Islands. First, we test the SVH using structural RS variables from light detection and ranging (LiDAR) and multispectral variables from a time series of Sentinel-2 images (S2). Since RS sensors can barely account for small, rare and understorey species, we expect that RS signals cannot adequately explain β-diversity that is derived from in-situ observations. This combination of data and techniques has not been used before to represent β-diversity with RS products. Second, we analyse to what extent β-diversity agrees with the pre-defined community types.

2 | METHODS

2.1 | Study region

The island of La Palma is located at the northwest edge of the Canary archipelago in the Atlantic Ocean, ca. 400 km west of the African coast at 28°N (Figure 1). The entire island is designated a 'UNESCO Man and the Biosphere Reserve'. La Palma is generally characterized by a subtropical-mediterranean climate. However, the elevational gradient and trade winds from the northwest constitute diverse climatic attributes leading to the existence of eight different ombrotypes, ranging from hyperarid to humid, within a small geographic extent (Garzón-Machado, Otto, & del Arco Aguilar, 2013).

2.2 | Field sampling

Field sampling was performed along the elevational gradient (from 45 to 2,400 m a.s.l.) present on the northwest part of the island, where anthropogenic pressure is low, semi-natural land cover is largely preserved, edaphic conditions are homogeneous (Carracedo,

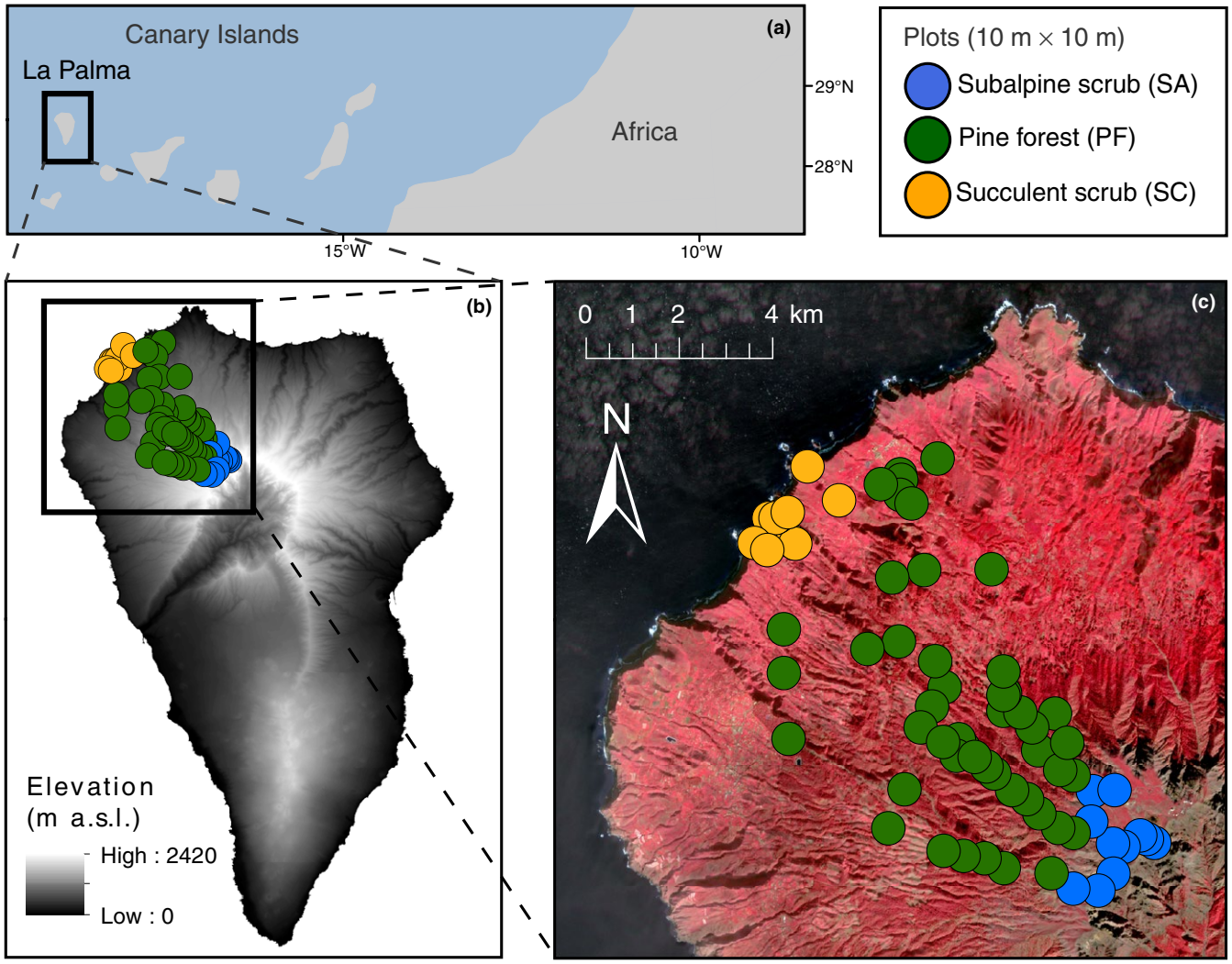

FIGURE 1 Location of sampling plots on La Palma, Canary Islands. (a) The Canary Islands are located in the Atlantic Ocean to the west of the African continent. (b) The entire island is a UNESCO Man and the Biosphere Reserve. The digital elevation model (Irl et al., 2015) shows the location of the sampling plots. The plots that include *Pinus canariensis* were classified as "Pine forest (PF)". Plots below the pine forest without *P. canariensis* were classified as "Succulent scrub (SC)", and plots above the pine forest without *P. canariensis* as "Subalpine scrub (SA)". (c) The false-colour composite image supports the visual interpretation of vegetation and is based on the Sentinel-2 imagery from 14 Jan 2017 with 10-m resolution (Band 8, Band 4 and Band 3)

Badiola, Guillou, De La Nuez, & Pérez Torrado, 2001) and human activities are scarce. Fieldwork was conducted during February and March 2017. Three main community types were crossed along elevation (Del Arco Aguilar, González-González, Garzón-Machado, & Pizarro-Hernández, 2010). Succulent scrublands occur in semi-arid conditions at low elevation (~0–500 m) and are dominated by *Euphorbia* scrub. The vegetation height can exceed 2 m. The vegetation cover is consistently high, but bare soil and rock can be found. The plant communities in mid-elevations are dominated by the endemic *P. canariensis*, which also forms the tree line both towards high and low altitudes (~500–2,000 m). The canopy cover and height peak in mid-elevation. The understorey consists of scrub species. The forest ground is covered with pine needles. The subalpine communities (~2,000–2,400 m) are characterized by the summit broom scrub *Adenocarpus viscosus* subsp. *spartioides* (hereafter *Adenocarpus viscosus*). The vegetation height barely reaches 2 m. Bare soil, rock and deadwood is frequently found in this vegetation zone. In accordance with Del Arco Aguilar et al. (2010), we pre-classified the sampling sites including *P. canariensis* as pine forest (PF), while those without *P. canariensis* below the pine forest were designated as succulent scrub (SC) and those above the pine forest were designated as subalpine (SA).

We applied a stratified random sampling along the elevational gradient. Thereby SC, PF and SA defined the strata. We avoided anthropogenic land use, northern slopes >20°, to prevent sites from being unnatural and appearing dark and distorted in remote sensing imagery. Due to ridges and steep slopes some sites appear linearly arranged (Figure 1). In each sampling site, a 10 m × 10 m plot was used to record plant community data. We sampled ten SC, 48 PF and 11 SA plots. We recorded abundances of all vascular plant species

within the plots, by estimating their coverage within three vertical strata (tree, scrub and herb layer). Since the presence of annual plants is driven by short-term weather events that differ locally, we only considered perennial plant species. The stochastic, short-term variation of the occurrence of annuals during the seasons makes it very difficult to conduct reliable comparisons with remote sensing data which are recorded at a different time. We used Muer et al. (2016) for the nomenclature of vascular plant species.

Since we are interested in changes of abundance-based species composition, we applied relative abundances to calculate β-diversity. Relative abundance per species and plot was calculated as the species' coverage divided by the sum of coverages of all species in all vertical strata. From this definition, we can accurately assess changes in species composition between plots, because land cover types other than vegetation (i.e. bare soil, rock and litter) that bias the β-diversity based on absolute abundances are neglected. If other cover types were considered, we would notice a reduction in absolute species abundances, even if the relative species abundances remain constant. However, such cover classes and the coverage of species influence the composition of RS signals. To perform an analysis of the composition of RS signals, we used the following explanatory variables: we estimated the absolute coverages of bare soil, rock, pine needles and deadwood that are not vertically covered by any other strata in the plot. In this RS-specific analysis, we also considered the absolute coverages of the ten most abundant species that are not covered by other strata. We refer to these coverages as 'RS-specific' coverages.

2.3 | Environmental data

Since mean annual temperature and mean annual precipitation are among the most important climate variables in community ecology at the landscape scale (Whittaker, 1970), we used them to characterize the plant communities in the study region. These climatic variables were generated by the interpolation of data from meteorological stations, applying linear regression kriging technique (for details see Irl et al., 2015). We extracted climate data for each plot from the grid by averaging the values of all climate cells that fall within the plot. In order to evaluate the human impact on species composition, we calculated for each plot the planar distance to the nearest anthropogenic infrastructure, i.e. roads and buildings of any kind (Figure S1 in Appendix S1).

2.4 | Remote sensing data

We considered RS products that represent multispectral and structural vegetation properties, and are thus appropriate to distinguish plant communities (Pettorelli et al., 2014; Xie, Sha, & Yu, 2008). To account for multispectral differences that may occur during the seasons, we selected 13 Sentinel-2 images (S2; European Space Agency 2017), covering the time period from February 2016 to February 2017 (Table S1 in Appendix S1). We chose S2, since this sensor provides images of high radiometric (12 bands), temporal (5 days revisit time) and spatial resolution (10–60 m) that are publicly available and free of charge (see https://sentinel.esa.int/documents/247904/685211/Sentinel-2_User_Handbook). The downloaded images were given as geometrically and radiometrically corrected Top-of-Atmosphere (TOA) Level-1C product. We applied atmospheric, terrain and bidirectional reflectance distribution (BRDF with cosine of local solar zenith angle) correction using the Sen2Cor plugin (see http://step.esa.int/main/third-party-plugins-2/sen2cor/) within the Sentinel-2 toolbox of the Sentinel Application Platform (SNAP) to generate Bottom-Of-Atmosphere (BOA) Level-2A products. These products include a masking layer for classifying pixels affected by clouds as "medium cloud probability", "high cloud probability" and "cirrus". The cloud mask covered a maximum of two plots per image (Table S1 in Appendix S1). Such plots were excluded from analyses. Band 1 (aerosol, 60 m), Band 9 (water vapour, 60 m) and Band 10 (cirrus, 60 m) were removed by the preprocessing procedure, as they are only needed for cloud-masking. The remaining bands are Band 2 (blue, 10 m), Band 3 (green, 10 m), Band 4 (red, 10 m), Band 5 (red edge, 20 m), Band 6 (red edge, 20 m), Band 7 (red edge, 20 m), Band 8 (near-infrared [NIR], 10 m), Band 8a (red edge, 20 m), Band 11 (shortwave infrared [SWIR], 20 m) and Band 12 (shortwave infrared [SWIR], 20 m).

We also applied basic vegetation indices to explore plant characteristics that lead to spectral differences. The normalized differentiation vegetation index (NDVI; [Band 8 – Band 4]/[Band 8 + Band 4]) is one of the most popular proxies for primary productivity (Pettorelli, 2013). Higher values of the moisture stress index MSI ([Band 11/Band 8]) reveal less leaf water content (Hunt & Rock, 1989). The plant senescence reflectance index PSRI ([Band 4 – Band 2]/Band 6) increases with canopy stress (carotenoid concentration), canopy senescence and fruit ripening (Merzlyak, Gitelson, Chivkunova, & Rakitin, 1999). The anthocyanin reflectance index ACR1 ([1/Band 3]/[1/Band 5]) demonstrates canopy changes through growth and death (Gitelson, Merzlyak, & Chivkunova, 2001). The carotenoid reflectance index CRI1 ([1/Band 2]/[1/Band 3]) represents carotenoid concentration relative to chlorophyll (Gitelson, Zur, Chivkunova, & Merzlyak, 2002); carotenoid pigments increase with vegetation stress. The photochemical reflectance index PRI ([Band 2 – Band 3]/[Band 2 + Band 3]) indicates light use efficiency (Gamon, Serrano, & Surfus, 1997); the PRI index changes with carotenoid pigments in live foliage and thus describes productivity and stress.

Metrics derived from airborne LiDAR are able to account for both 2D and 3D vegetation structure, which helps to distinguish vegetation that differs in structural variables such as growth height and canopy cover (Pettorelli et al., 2014). Airborne laser scanning (ALS) point cloud data from April 2009 was downloaded from the Spanish National Geographic Institute (IGN). The point clouds have a density of 0.5 points per 1 m^2 (see Appendix S2). After data pre-processing, several indices were calculated with a grain size of 20 m. The canopy height model (CHM) returns the average of normalized heights above ground. The tree fraction cover (TFC) is the proportion of first ALS returns over 2 m above ground from the total amount of first ALS return in the raster cell. The vegetation fraction (VF) reflects the number of all returns over 0.5 m height divided by the number of all returns within the cell. The

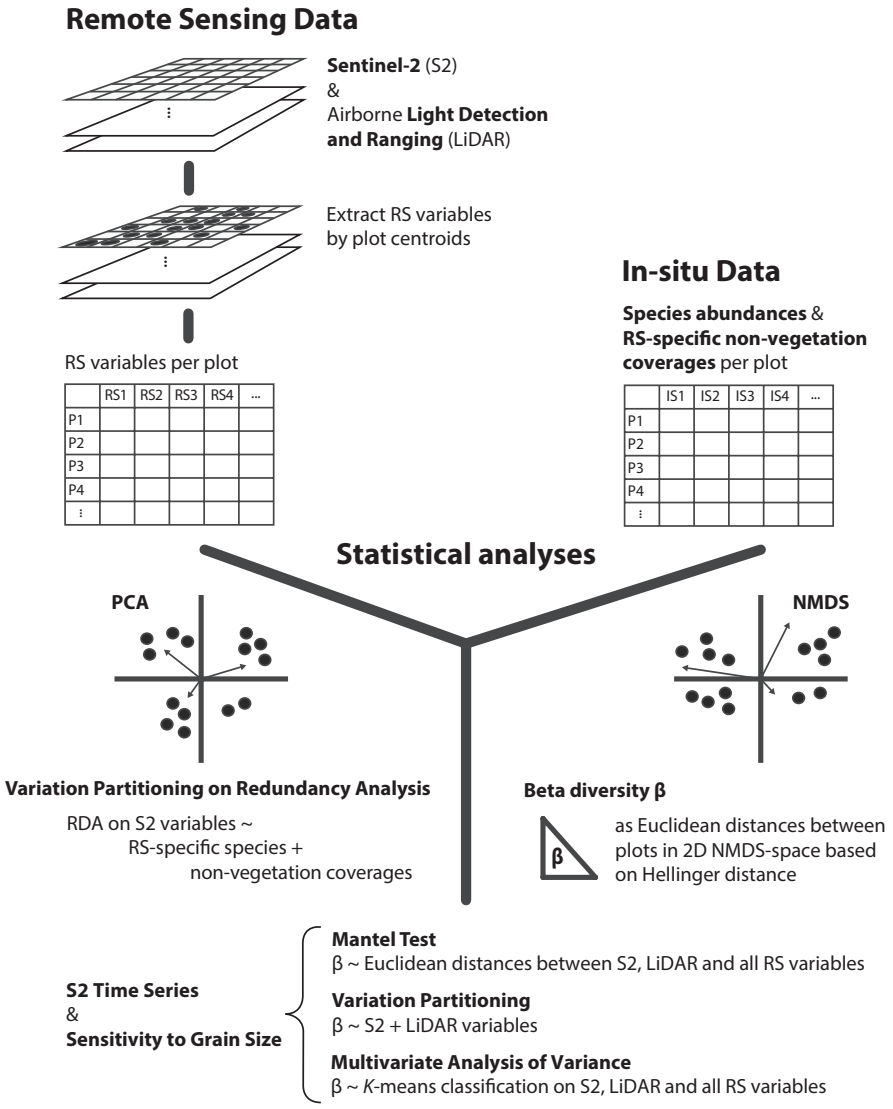

FIGURE 2 Flow chart describing the remote sensing and in-situ data as well as the statistical analyses to evaluate the relationship between the two. For details see Methods section.

return proportion (RP) indices were calculated as the number of ALS returns in different vertical strata (0.5, 2, 5, 10, 15, 20, 25 m) divided by the total number of ALS returns in the cell. Thus, RP provides information about the 3D vegetation structure. The effective leaf area index (LAI) was computed based on the gap probability, but not corrected for woody elements or the clumping effect. For classifications based on RS data all variables were standardized to zero mean and unit variance. In order to retrieve (pair-wise) distances between plots based on these standardized RS variables, we applied the Euclidean distance measure.

To reduce the bias induced by GPS inaccuracy when extracting the RS data by plot centroids, we use RS metrics with a minimum grain size of 20 m. In addition, we evaluated the sensitivity of results to coarser grain sizes (40 and 60 m) by aggregating the RS metrics, i.e. taking the mean value.

2.5 | Statistical analyses

Our methodological approach to analyse the relationship between in-situ and RS variables is summarised in Figure 2. To describe the given plant communities and demonstrate the species' realized environmental niches, we modelled the coenoclines of the ten most abundant species. A coenocline is a response curve of the species abundance along a single gradient (Whittaker, 1967). Species with overlapping coenoclines form communities. We applied two environmental gradients: mean annual temperature and mean annual precipitation. Coenclines were generated by fitting generalized additive models (GAM) with Gaussian distribution and link function, and thin plate regression splines as the single penalty smooth class (Wood, 2017). Because we were facing unequal sample sizes between community types, we conducted non-parametric Kruskal-Wallis ANOVA (Siegel & Castellan, 1988) to identify differences in species richness (Figure S2 in Appendix S1). Linear regression models were applied to determine the relationship between species richness and environmental gradients. Model assumptions were verified visually.

Beta-diversity can be understood as the dissimilarity between plots regarding their species composition (Whittaker, 1967). We applied non-metric multidimensional scaling (NMDS) to assess β-diversity and distinguish plant communities (Legendre & De Cáceres,

2013). The NMDS is a distance-based, indirect ordination technique. We avoided direct ordination methods, since we were interested in unconstrained results that only rest on compositional dissimilarity (McCune & Grace, 2002). The NMDS ranks distances between input data (plots); therefore, NMDS bypasses the linearity assumptions of metric ordination methods. Here we applied Hellinger distance to calculate the distance matrix among plots regarding their species composition (Legendre & De Cáceres, 2013). The Hellinger distance down-weights the occurrence of rare species. Thus, we controlled for overrated influence of rare species in dissimilarity calculations. We calculated a 2D ordination space running 100 attempts and involving random starting configurations, to find the optimal solution by NMDS, i.e. the lowest stress value. The NMDS-space was rotated to principal components; most variation in the data is shown along the first axis, followed by the second. We conducted post-hoc correlation of explanatory variables to the NMDS via surface and vector fitting, to interpret the influence of explanatory variables onto the compositional dissimilarity represented by the location of plots in the NMDS-space. We eventually calculated β-diversity as the Euclidean distances between plot locations in the 2D NMDS space.

Subsequently, we utilized the Mantel test (Mantel, 1967) to quantify the correlation between β-diversity and the pair-wise distances between plots based on RS variables. Moreover, variation partitioning was used to reveal the combined and independent effects of S2 and LiDAR variables explaining the β-diversity (Legendre & Anderson, 1999). Variation partitioning is based on a redundancy analysis (RDA), linearly modelling the relationship between a set of dependent variables and two sets of explanatory variables. We also employed *K*-means unsupervised classification algorithm (Lloyd, 1982) to distinguish three community types considering RS variables only. We aimed to create three classes, because existing vegetation maps predefine three main community types in the study region: succulent scrub, pine forest and subalpine scrub. The *K*-means algorithm has been used before to test the SVH (Schmidtlein & Fassnacht, 2017). We then conducted MANOVA (Anderson, 2001) to estimate how *K*-means classification on RS variables fits to the β-diversity.

The Mantel test, variation partitioning and MANOVA was applied to each S2 image as well as to the mean, range (|max−min|) and *SD* of all dates. We can consequently identify seasonal variation of the explanatory power of RS signals, and account for complementarity of RS signals over time. This time series analysis was also conducted separately for each of the three vegetation types. Here we only applied the Mantel test, since the sampling size of SC and SA was too small to apply variation partitioning, and the MANOVA requires

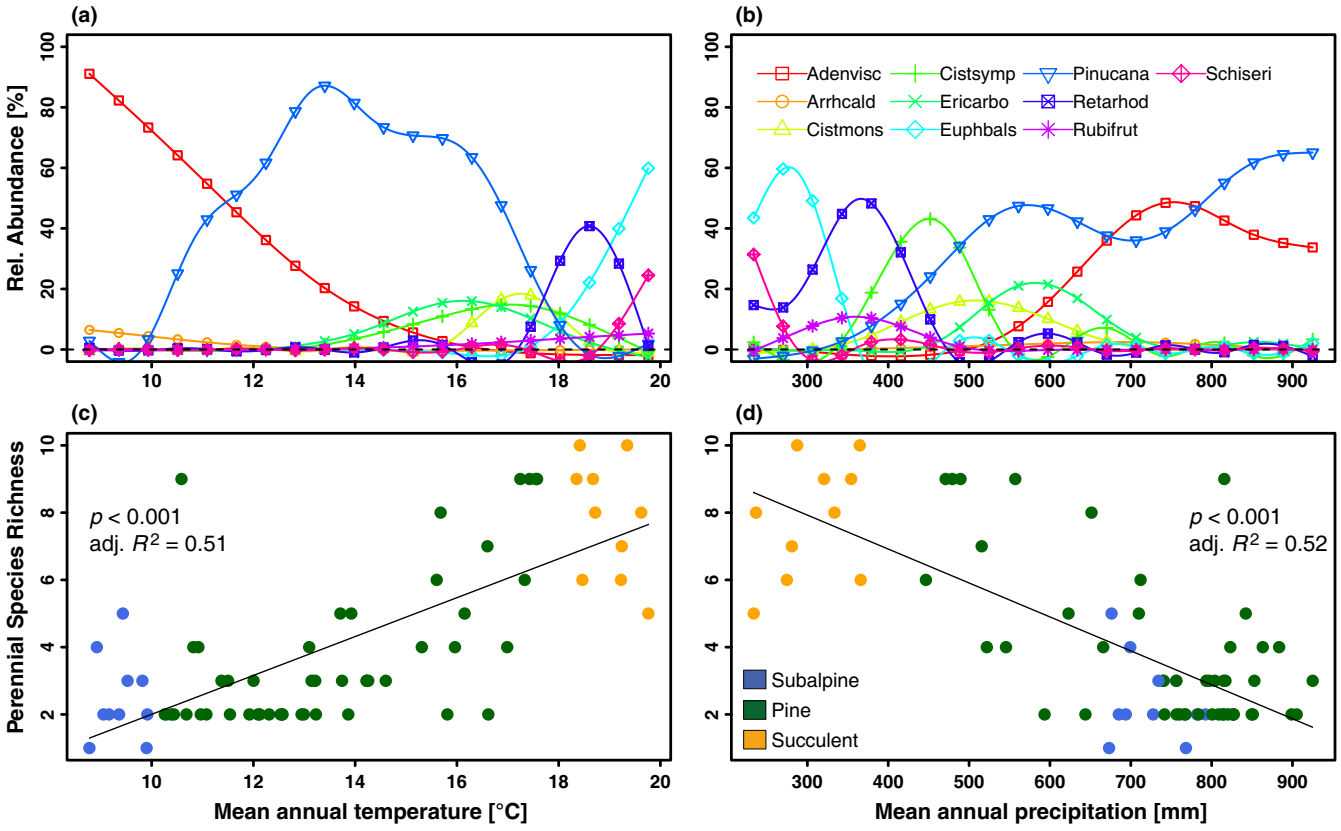

FIGURE 3 Species abundance vs. environmental gradients. GAM indicate the relative abundance of the ten most abundant species in the data set for (a) mean annual temperature, and (b) mean annual precipitation. The linear regression model demonstrates the relationship between (c) perennial species richness and mean annual temperature, and between (d) perennial species richness and mean annual precipitation. Species abbreviations: *Adenocarpus viscosus* (Adenvisc), *Arrhenatherum calderae* (Arrhcald), *Cistus monspeliensis* (Cistmons), *Cistus symphytifolius* (Cistsymp), *Erica arborea* (Ericarbo), *Euphorbia balsamifera* (Euphbals), *Pinus canariensis* (Pinucana), *Retama rhodorhizoides* (Retarhod), *Rubia fruticosa* (Rubifrut), *Schizogyne sericea* (Schiseri)

vegetation classes, which is pointless to produce within single community types. The β-diversity within vegetation types was thereby again given by the point distances in the NMDS that involves all plots (see above).

Furthermore, we applied a PCA (Mardia, Kent, & Bibby, 1979) to the RS variables, but used the S2 variables from the S2 image that showed the highest mean of the three correlational results from the Mantel test, variation partitioning and MANOVA. We thus illustrate the variation in RS signals that can best explain β-diversity and depict the RS products that add most to this variation. As for the NMDS, we added post-hoc correlation of explanatory variables via vector fitting. In addition, variation partitioning onto an RDA was used to separate the variation among these date-specific S2 variables that can be explained by RS-specific coverages of the ten most abundant species and of non-vegetation cover types (i.e. bare soil, rock, pine needles and deadwood).

Data processing and statistical analyses were conducted using open-source R Statistics (R Foundation for Statistical Computing, Vienna, Austria; v 1.0.136) and corresponding default settings, if not mentioned differently (Table S2 in Appendix S1).

3 | RESULTS

The responses of the ten most frequent perennial plant species to the major climatic gradients are clear and unimodal (Figure 3a,b). In the semi-arid conditions of the low elevation zone, several species associated with succulent communities show maximum performance with the highest temperature and lowest precipitation along the elevation gradient (*Euphorbia balsamifera*, *Retama rhodorhizoides*, *Rubia fruticosa*, *Schizogyne sericea*). *Cistus monspeliensis*, *C. symphytifolius* and *Erica arborea* become more abundant with decreasing temperature and increasing precipitation. They share their realized environmental niches with *P. canariensis*, which is most abundant at a mean annual temperature of ca. 14°C and at the highest annual precipitation found in the region (~925 mm). In the subalpine communities, *Adenocarpus viscosus* and *Arrhenatherum calderae* show maximum abundance with decreasing precipitation and lowest temperatures.

Species richness is also clearly related to climatic variables, namely a positive relationship with temperature and a negative relationship with rainfall (Figure 3c,d). Despite these significant relationships, the three main vegetation types are clearly identified in the species richness vs. temperature graph, but not in the species richness vs. rainfall graph, which is explained by a rainfall decrease at high elevations. We did not detect a significant relationship between the relative abundance of *P. canariensis* and perennial species richness (not shown), but the SC plots harbour considerably more species than both other classes (Figure S2 in Appendix S1).

Figure 4a reveals that the S2 variables from 14 Jan 2017 (20-m grain size) correlate on average most strongly with the β-diversity. We additionally observe a "W"-shape; the correlation between S2 variables and β-diversity is stronger during the wet (Dec–Mar) and dry season (Jun–Sept), compared to other months. The multitemporal analysis demonstrates that neither the mean nor the range and *SD* of the time series reaches the highest correlation results of single image dates (Figure 4b). Here the multitemporal mean of S2 variables yields on average the strongest correlation with β-diversity, compared with the multitemporal range and *SD*. Interestingly, the multitemporal MANOVA results are weakest of the three statistical tests, but for single dates the two strongest correlations are produced by MANOVA (Figure 4a). The Mantel test reveals a r_{RS} = 0.41 (p < 0.001) considering all RS variables from 20-m resolution data (Figure 4c).

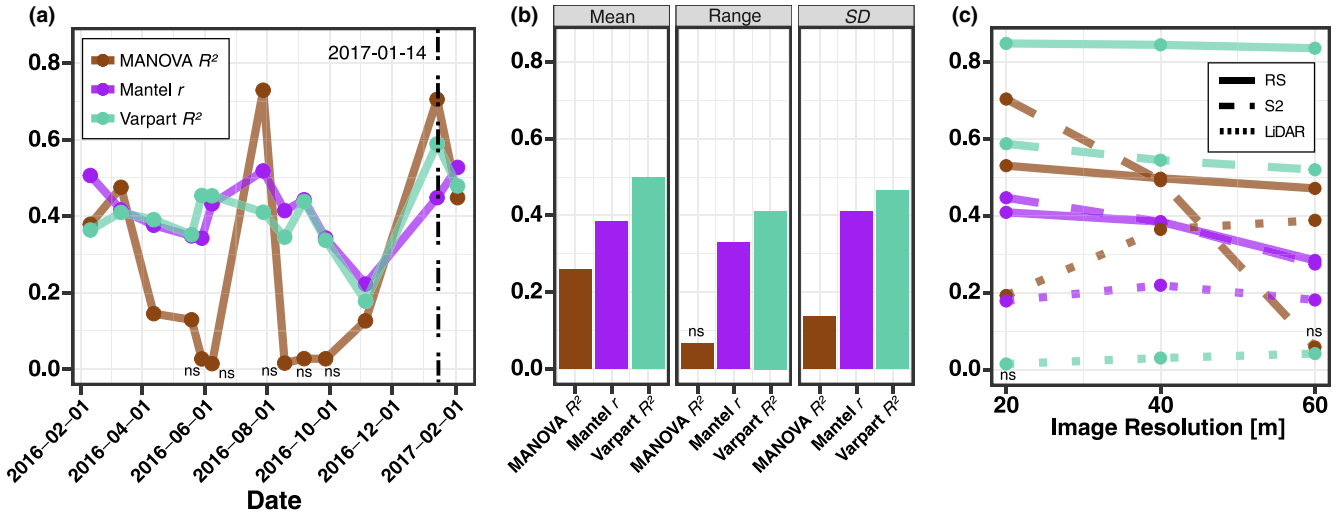

FIGURE 4 Time series analysis of Sentinel-2 (S2) images and sensitivity analysis concerning grain size. In (a) the date-specific correlation results between the S2 variables of 13 images (20-m grain size) and the β-diversity are shown. Part (b) shows the correlation results applying the multitemporal mean, range (|max-min|) and *SD* of the time series of S2 variables. The S2 image from 14 Jan 2017 indicates the strongest correlation from the three statistical tests (MANOVA, Mantel test, variation partitioning). This S2 image was used for the sensitivity analysis in (c). Here, we show the statistical results for coarser grain sizes (40 and 60 m) by aggregating the RS-derived metrics (i.e. taking the mean value). "Ns" highlights non-significant ($p \geq 0.05$) correlation results

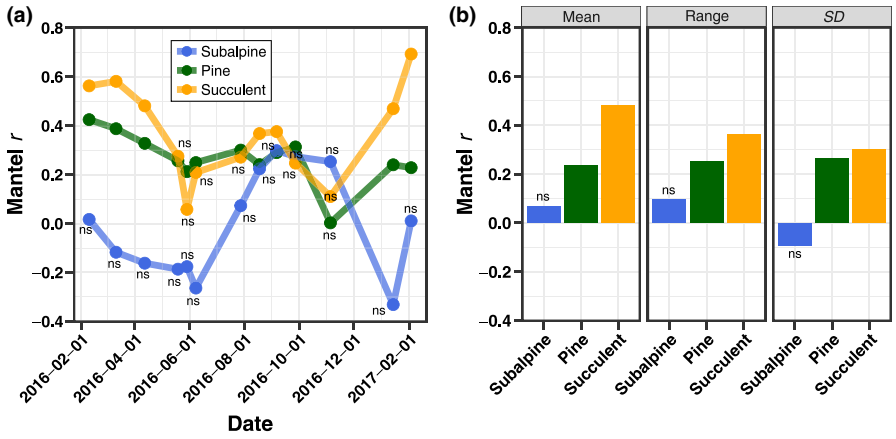

FIGURE 5 Time series analysis of Sentinel-2 (S2) images, separated by community type. In a) the date-specific Mantel correlations between the S2 variables of 13 images (20-m grain size) and the β-diversity of the subalpine, pine and succulent community are shown. Part b) demonstrates the Mantel correlation results between the mean, range (|max-min|) and *SD* of the time series of S2 variables and the β-diversity of the three community types. "Ns" highlights not significant ($p \geq 0.05$) correlation results

Considering only LiDAR variables, yields a Mantel r_{LiDAR} of 0.18 ($p = 0.008$). Variation partitioning of β-diversity through a combination of S2 and LiDAR variables (20-m grain) leads to a total R^2_{Rs} of 0.85 ($p < 0.001$). The R^2_{S2} resulting from independent effects of S2 signals is 0.59 ($p = 0.001$). The R^2_{LiDAR} of the independent effect of LiDAR signals is 0.01 and not significant ($p = 0.111$). The combined effects of S2 and LiDAR variables produce $R^2_{S2+LiDAR} = 0.25$. Accordingly, $R^2_{S2} + R^2_{LiDAR} + R^2_{S2+LiDAR} = R^2_{Rs} = 0.85$. Applying the *K*-means classification algorithm to all RS variables leads to differentiation of three classes that moderately explain the dissimilarities in species composition (Figure 4c; MANOVA: $p < 0.001$, $R^2_{Rs} = 0.53$). When considering S2 variables only (Figure 4c), *K*-means classification outcomes adequately reflect the β-diversity ($p < 0.001$, $R^2_{S2} = 0.70$). A classification solely based on LiDAR variables yields a worse fit (Figure 4c; $p = 0.001$, $R^2_{LiDAR} = 0.19$). The correlation results between S2 variables and β-diversity decrease with increasing grain size (low resolution), while for LiDAR variables the correlation slightly increases (Figure 4c). Except for variation partitioning, the statistical tests reveal that the correlation between all RS variables and β-diversity among 10-m plots is strongest for 20-m grain size, but resulting differences in explanatory power between grain sizes can be marginal.

Separating the time series analyses by vegetation types resulted in Figure 5. In particular, SC undergoes temporal variation in S2 signals and shows highest Mantel *r* among communities, followed by PF and SA (Figure 5a); the SA correlations also cover a wide range and even became negative, but were not significant due to low sample size and very homogeneous S2 signals; the "w"-shape is less clear for PF. The multitemporal mean of the time series produces the strongest correlation for SC, followed by the multitemporal range and *SD* (Figure 5b); for PF, this is the opposite.

The NMDS based on the species abundances (Stress = 0.06) demonstrates no clear distinction between PF and SA (Figure 6a). At lower altitudes, a considerable gap between PF and SC does become obvious. Consequently, the similarity in species composition between SA and PF is considerably higher than between SC and PF. Within PF we find emphasized compositional variation in the lower part close to the transition to SC. Such variation along the second NMDS axis also appears in the subalpine zone. The relationship between β-diversity and nearest distance to anthropogenic land use is very weak (Figure S1 in Appendix S1). We focus in the following on RS variables derived from RS data at 20-m spatial resolution from the S2 image acquired on 14 Jan 2017; among these RS variables, Band 3, Band 5, Band 6, Band 7, Band 8, Band 8a, NDVI, PSRI, MSI, RP0.5m, RP2m, RP5m, RP10m, LAI and VF correlate significantly ($p < 0.05$) with the NMDS scores (Figure 6a; for details see Table S3 in Appendix S1). These variables are mostly associated with the second NMDS axis, which accounts for less β-diversity than the first axis. Canopy stress, senescence or fruit ripening (PSRI), water stress (MSI) and productivity (NDVI) are associated with the first NMDS axis.

The PCA based on RS variables shows that both axes contribute to the differentiation of vegetation types (Figure 6b), but the three communities appear less clearly separated than for the species data (Figure 6a); the distances between SC, PF and SA are not as pronounced as in the species-based NMDS ordination. Increasing S2 band values are mostly related to SC. The majority of LiDAR metrics increase along PF plots. Weakening vegetation, canopy growth or death (CRI1, ACR1), and productivity (NDVI) are also associated with the pine community. Light use efficiency (PRI), water stress (MSI) as well as canopy stress, senescence or fruit ripening (PSRI) accompany SA plots. The structural variable RP0.5m is related to SA, whereas RP2m reflects SC. The PCA axes loadings of the RS variables are given in Table S4 (Appendix S1). Among the other explanatory variables, only the RS-specific coverage of *Cistus monspeliensis*, *C. symphytifolius* and *Erica arborea* are not significantly correlated with the PCA scores (Table S3 in Appendix S1). The RS-specific coverage of the other species is correctly linked to their corresponding communities. RS-specific coverage of deadwood is linked to SA, of rock and bare soil to SC as well as to SA.

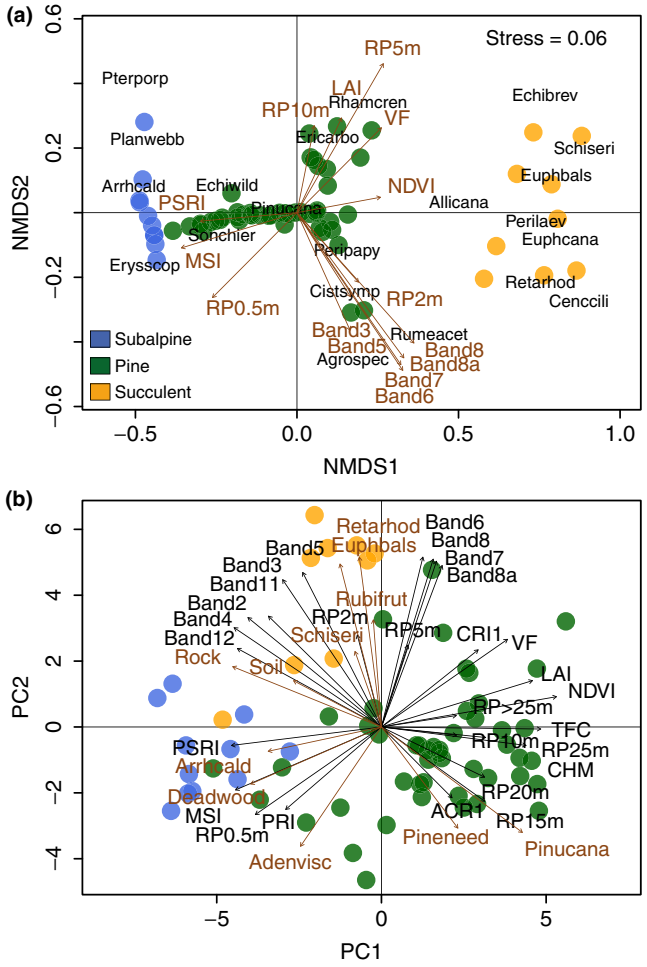

FIGURE 6 The location of plots in the 2D ordination space calculated via NMDS and PCA. (a) The PC-rotated NMDS space represents β-diversity calculated by the Hellinger distance between plots, considering the abundances of perennial plant species. The NMDS-stress value of 0.06 shows a good fit. (b) The PC-rotated PCA space is calculated by the remote sensing (RS) variables derived from the Sentinel-2 image taken on 14 Jan 2017. A proportion of 60% of total variance is explained by PC1 (39%) and PC2 (21%; for details see Table S4 in Appendix S1). The vectors of explanatory variables (brown arrows) and PCA-input variables (black arrows) were fitted after generating the ordination space (for details see Table S3 in Appendix S1). Species abbreviations: *Adenocarpus viscosus* (Adenvisc), *Agrostis* spec. (Agrospec), *Allium canariense* (Allicana) *Arrhenatherum calderae* (Arrhcald), *Cenchrus ciliaris* (Cenccili), *Cistus symphytifolius* (Cistsymp), *Echium brevirame* (Echibrev), *Echium wildpretii* (Echiwild), *Erica arborea* (Ericarbo), *Erysimum scoparium* (Erysscop) *Euphorbia balsamifera* (Euphbals), *Euphorbia canariensis* (Euphcana), *Periploca laevigata* (Perilaev), *Pericallis papyracea* (Peripapy), *Pinus canariensis* (Pinucana), *Plantago webbii* (Planwebb), *Pterocephalus porphyranthus* (Pterporp), *Retama rhodorhizoides* (Retarhod), *Rhamnus crenulata* (Rhamcren), *Rubia fruticosa* (Rubifrut), *Rumex acetosa* (Rumeacet), *Schizogyne sericea* (Schiseri), *Sonchus hierrensis* (Sonchier)

Furthermore, variation partitioning onto the RDA explaining the variation in RS variables leads to a total R^2_{Total} of 0.62 ($p = 0.001$), which is the sum of the effects of the RS-specific coverages of species and non-vegetation types (rock, bare soil, deadwood, pine needles): $R^2_{Total} = R^2_{Species} + R^2_{Non-vegetation} + R^2_{Species + Non - vegetation}$. Thereby, RS-specific species coverages independently account for an $R^2_{Species}$ of 0.29 ($p = 0.001$), whereas the independent effect of non-vegetation coverages scores a non-significant ($p = 0.067$) $R^2_{Non-vegetation}$ of 0.05. The combined effects of vegetation and non-vegetation coverages result in $R^2_{Species+Non-vegetation} = 0.28$.

4 | DISCUSSION

4.1 | Beta-diversity and remote sensing signals

Contrary to our initial expectations, we show that a combination of multispectral and structural RS variables can explain up to 85% of β-diversity in the plant communities of the study system. The S2 variables constitute more explanatory power than the LiDAR variables we selected. These outcomes are partly in line with similar studies that considered different variables and scales. He, Zhang, and Zhang (2009) quantified the relationship between NDVI distances (derived from MODIS with 250-m resolution) and plant β-diversity (using pair-wise Bray-Curtis dissimilarity) within entire US counties. The highest Mantel *r* was achieved at the species level ($r = 0.4$); see He and Zhang (2009) for a similar approach at the global scale. Hall, Reitalu, Sykes, and Prentice (2012) used multispectral variables derived from QuickBird imagery with a grain size of 2.4 m. They applied variation partitioning on grassland β-diversity (local-to-regional richness ratio), sampled in 0.5-m plots representative for larger sites, which resulted in an R^2 of 0.27 for the independent effect of multispectral RS variables. That is lower than the explanatory power we found, although their study scale was much smaller.

Indeed, the different extents of pixels and plots affect the correlation between RS signals and β-diversity. On the one hand, pixels larger than the plot extent imply a mixture of spectral signals that do not only originate from the plot extent (Nagendra, Rocchini, Ghate, Sharma, & Pareeth, 2010). On the other hand, applying a sampling design with pixels smaller than the plot extent implies either sampling vegetation in larger plots or to using RS data with higher spatial resolution (Rocchini et al., 2010). Plots larger than 10 m × 10 m are rarely applied in vegetation ecology, because the sampling effort is large, particularly in open vegetation types (Chytrý & Otýpková, 2003). Moreover, Rocchini (2007) found a Mantel *r* of 0.69 for the correlation between species diversity sampled in 10 m × 10 m plots and QuickBird data with much smaller spatial resolution (3 m). This Mantel *r* is not considerably larger than our findings; in the case of over-sampling (i.e. plots larger than pixels) high-resolution data may contain a considerable amount of noise (Nagendra & Rocchini, 2008), even though the species composition of pixels may be inaccurate in the case of under-sampling (i.e. plots smaller than pixel). An increase in spectral resolution can also compensate for low spatial resolution (Rocchini, 2007).

Usually, communities that are subject to climate seasonality can be well separated by RS data (Horning, Robinson, Sterling, Turner, & Spector, 2010). During the wet (Dec to Mar) and dry (Jun to Sept)

season, multispectral variables correlate more strongly with the dissimilarity in species composition than in other months. The multitemporal variables, however, cannot explain the same amount of β-diversity as date-specific variables at maximum. This offers potential for further investigations, exploring the explanatory power of date-specific multispectral variables and vegetation indices to detect the reasons behind these findings. We assume that the dominant and stem-succulent species of the succulent zone, such as *Euphorbia balsamifera* and *Euphorbia lamarckii*, shed their leaves in the dry season (Muer et al., 2016). In addition, understorey species of the pine forest and subalpine species frequently show discolouration during dry spells. The highly abundant bright yellow flowers of the dominating *Adenocarpus viscosus* might also lead to multispectral differentiation of subalpine vegetation in June (Muer et al., 2016). Furthermore, during the wet season, ice storms can cause discoloration of *Adenocarpus viscosus* as a result of leaf tissue damage (Palomares Martínez et al., 2011).

In January, as our date-specific PCA showed the vegetation indices PSRI, MSI, PRI, ACR1 and CRI1 may represent vegetation stress. Especially the high-elevation pine and subalpine community experience freezing temperatures and low precipitation. Trade winds prevent the orographic and convective rise of moist air, leading to aridity also in the subalpine zone throughout several months (González Henríquez, Rodrigo Pérez, & Suárez Rodríguez, 1986). The trade wind cloud facilitates fog drip. The high reflectance of red light (i.e. Band 4, Band 5 and PSRI) was mostly associated with the succulent and subalpine scrub. This is an indicator for low leaf pigment content and small leaf area, as well as brown rock, soil and litter (Frampton, Dash, Watmough, & Milton, 2013). In addition, leaf water content is positively related to chlorophyll content (Sims & Gamon, 2002). Thus, leaf water content (i.e. MSI) of the succulent and subalpine scrub may be low due to aridity resulting in less chlorophyll and higher reflectance. Another reason for high reflectance in the visible spectrum refers to succulent leaf thickness, which prevents light penetration and absorption of lower leaf layers (Sims & Gamon, 2002). High NDVI values correspond to the pine forest, where annual precipitation is highest, probably indicating high biomass production. Most LiDAR-derived structural variables represent the physiognomic forest structure very well (Ørka, Wulder, Gobakken, & Næsset, 2012; Rees, 2007). The association of structural variables representing different heights above ground (RP variables) with the community types in the date-specific PCA agrees with observed vegetation heights in the field.

In our study multispectral S2 variables explain β-diversity more accurately than structural LiDAR variables. One reason is that the vegetation coverages of both scrub types are similar and characterized by rocky outcrops and bare soil. Considering additional LiDAR metrics that particularly differentiate the vertical scrubland structure between 0.5 and 2.0 m may lead to a stronger correlation between LiDAR products and β-diversity. Besides, the LiDAR data were acquired in April 2009. Since then perennial plant coverage and structure may have changed slightly. However, increasing grain size results in increasing explanatory power of LiDAR variables applying MANOVA, while explanatory power of S2 variables decreases in all statistical tests. The low LiDAR point density and thus high variation (noise) in LiDAR variables could be responsible for weak correlations with β-diversity at small scales (20 m). The noise is reduced by averaging pixel values, i.e. with increasing extent the LiDAR metrics become more stable. Hence, the average structural signatures of entire community types are rather reflected by relatively large grain sizes (60 m), which then lead to more distinct LiDAR-based classes in *K*-means clustering that correlate stronger with β-diversity.

A proportion of 62% of variation in S2 signals from 14 Jan 2017 can be explained by RS-specific coverages of species and non-vegetation cover, but the RS-specific coverages of bare soil, rock and litter barely add to the differentiation of plots based on S2 signals alone. 38% of variation in S2 variables can neither be explained by the species coverages, nor by non-vegetation cover types, probably because of differing spatial extents of plots and pixels and GPS location bias.

The GPS inaccuracy affects the co-location of RS and in-situ data. For S2 imagery, a GPS location error of 3, 6 and 18 m is given for 10-, 20- and 60-m bands, respectively (Baillarin et al., 2012). Due to the field sampling conditions (i.e. cloud-free, no northern aspects, slope <20°, no obstacles), the GPS accuracy of the plot locations could be reduced to a mean of 3.6 m (±1.0 m *SD*). However, the cardinal direction of the true location shift remains unknown. Thus, a total GPS error of 6 m for 20-m bands plus the GPS error of the plot locations is possible and likely to cause unexplained variation when correlating RS with in-situ data. However, as the sensitivity analysis shows, the GPS bias seems minor, since the lowest grain size of 20 m yields equally high correlation results compared to 40 and 60 m.

The moderate conformity of RS-based classes with the β-diversity pattern reveals that both sets of variables, S2 and LiDAR, are able to reclassify the pine forest plots, even though unsupervised classifications may be less accurate than supervised techniques (Horning et al., 2010). The two sets seem to contradict each other, because the explanatory power decreases when it comes to defining vegetation classes considering a combination of the two sets. Therefore, increasing the number of RS variables does not necessarily lead to more variation explained.

The RS data were not able to totally resolve the community types and β-diversity in this semi-natural system, which suggests similar RS properties of different species assemblages. Understorey species may be highly abundant and determine β-diversity, but are not detectable for RS sensors. In the case of heterogeneous, yet distinct, plant communities that comprise the same spectral signals (Sha, Bai, Xie, Yu, & Zhang, 2008), the potential of RS approaches in vegetation science is limited.

4.2 | Species richness and β-diversity

Many studies describe continuous change in plant composition along an elevational gradient (Auerbach & Shmida, 1993; Enright, 1982; Hamilton, 1975; Ogden & Powell, 1979; Whittaker, 1956). In contrast, we identified two very distinct communities at low altitudes

– succulent scrub and pine forest – even though the main environmental gradients do not change abruptly. The sharp ecotone appears with the presence of the Canarian endemic *Pinus canariensis*. Other ordination-based studies also reveal discontinuities in compositional patterns with the increasing dominance of a key tree species (Druitt, Enright, & Ogden, 1990; Walker & Guppy, 1976), inducing positive feedback switches (Wilson & Agnew, 1992); *P. canariensis* influences environmental resources (e.g. water, light and nutrient availability), so that thermophilic species such as *Euphorbia balsamifera* and *Retama rhodorhizoides* do not establish in the forest understorey. This is associated with selection, a major process shaping species communities, results from fitness differences and interactions between species and the environment (Vellend, 2010).

Shade-tolerant species such as *Erica arborea* and *Myrica faya* do, however, occur under humid conditions in the lower pine forest, but not in the arid conditions of the upper succulent zone. We expected a continuous transition in species composition between the succulent and the pine community, according to the distribution of *Cistus monspeliensis* and *Cistus symphytifolius* that occur in open forest stands of low elevation as well as in the upper succulent zone. However, their abundances are too low to substantially increase compositional similarity in the lower ecotone. In contrast, the leguminous and light-demanding shrub *Adenocarpus viscosus* that dominates above the tree line is also abundant in open *P. canariensis* stands at higher elevations. Consequently, the similarity in species composition between the pine forest and the subalpine zone is much higher than between the pine forest and the succulent scrub. This is in agreement with Hamilton and Perrott (1981), who conclude that, along elevation gradients, lower community limits are strongly influenced by competition, whereas upper limits are mostly climatically determined.

We propose that the sharp community boundary also results from different species pool sizes. Species pool size is generally smaller at higher elevation due to lower speciation rates (Ricklefs, 1987) and decreasing area with elevation (Karger et al., 2011). Dissimilarity in species composition intrinsically increases with richness differences between species assemblages, because the chance of species overlap decreases (Anderson et al., 2011). At the upper tree line, only about three perennial vascular plant species are present, whereas approximately eight species occur at the lower transition zone. Furthermore, species richness strongly decreases from the succulent scrub to the pine forest, but stays constant from the pine forest to the subalpine scrub. Hence, β-diversity is enhanced across the lower tree line, not only due to species replacement, but also due to richness differences.

The strict separation between the succulent and the pine forest community might also be explained by a difference in disturbance regimes, which influence selection (Lawton, 1999), but also speciation in evolutionary time spans (Vellend, 2010). Regular occurrence of fire is common in the Canary pine forest ecosystem (Climent, Tapias, Pardos, & Gil, 2004); fire sometimes spreads into the subalpine zone (Irl et al., 2014). Contrary to thermophilic species of the succulent vegetation, *P. canariensis* and understorey species display adaptations to fire (pyropyhtes). *P. canariensis* produces epicormics shoots and basal sprouts, and serotinous cones release seeds after fire events (Climent et al., 2004). Understorey species such as *Myrica faya*, *Erica arborea*, *Cistus symphytifolius*, *Cistus monspeliensis* and *Adenocarpus viscosus* regenerate quickly after fire events (Höllermann, 2000). From field observations (burned area) and literature reviews (Climent et al., 2004; Méndez et al., 2015; Molina-Terrén, Fry, Grillo, Cardil, & Stephens, 2016), short-term fire regimes do not vary among plots and long-term forest regeneration does not depend on the fire regime either (Méndez et al., 2015). Consequently, the fire regime might explain the strong compositional differentiation between pine forest and succulent scrub due to the selection and speciation of species being differently adapted to fire (Arévalo, Fernández-Palacios, Jiménez, & Gil, 2001).

Furthermore, the European rabbit (*Oryctolagus cuniculus*), feral goat (*Capra hircus*) and Barbary sheep (*Ammotragus lervia*), introduced mammals on La Palma, induce the dominance of *Adenocarpus viscosus* at high elevation (Irl et al., 2012). Moreover, anthropogenic land use influences pine forest diversity at lower altitudes (Vellend et al., 2007). Thinning of *P. canariensis* plantations for timber production enhances habitat heterogeneity, understorey species diversity, seed production and regeneration of *P. canariensis* (Otto, García-del-Rey, Méndez, & Fernández-Palacios, 2012). Although we did not find evidence for recent anthropogenic impacts, the legacy of such disturbance regimes can act over decades (Vellend et al., 2007). In any case, fire and herbivory likely contribute to the decline of species richness with elevation in the study region (Irl et al., 2015), despite precipitation increase, since rabbit densities can be high above the tree line (Cubas et al., 2018). Thus, decreasing richness differences may reduce β-diversity between the subalpine and pine community.

The vague community boundary between the pine forest and the subalpine scrub raises questions about the existence of two distinct communities. Community and ecotone definition are a matter of scale (Hufkens et al., 2009; Ricklefs, 2008). Here we apply a regional approach that does not consider transition at local scale nor through time. Moreover, we did not test for causal mechanisms determining compositional (dis-)continuities (Shipley & Keddy, 1987). From a physiognomy point of view, the tree line may indicate the community limit, but in terms of species composition, limits are unclear (Walker et al., 2003). Often boundaries are human constructs. Lines on a map drawn between ecoregions do not implicitly correspond with any obvious physical discontinuities in nature (Strayer, Power, Fagan, Pickett, & Belnap, 2003). Because fundamental environmental gradients were adequately covered by the plots, and the relationship between β-diversity and nearest distance to anthropogenic land use was very weak, these outcomes are unlikely to be caused by sampling bias or human influence.

5 | CONCLUSION

Our study demonstrated the potential of multiple RS products to represent patterns in plant community composition over large extents, in a short time and at low cost. In-situ sampling was indispensable to precisely determine and understand β-diversity and community

distinction. The degree of concordance between spectral and β-diversity depends not only on the studied system, but also on the methods applied (Schmidtlein & Fassnacht, 2017). Such methods that identify and map discontinuities in β-diversity are necessary for conservation planning and wildlife management (Socolar et al., 2016).

On the one hand, spatial and temporal resolution of RS data may limit the potential of linking field observations with RS data, since interaction between species and environment may occur at scales finer than those RS can deliver. In such cases, other techniques than those applied here may be appropriate (e.g. high spatio-temporal and hyperspectral resolution, space-borne LiDAR), but most high-quality RS data are costly. On the other hand, in-situ data are also often missing. Facing these limitations, project collaborations are necessary to bring together scientists from ecology and remote sensing to exploit the vast potential of a combination of in-situ data and earth observation for science and conservation practice.

ACKNOWLEDGEMENTS

We acknowledge help from Marie-Isabell Lenz during the field campaign.

AUTHOR CONTRIBUTIONS

S.H. and T.S. collected the field data and processed the Sentinel-2 images. M.A.T., S.M. and A.B. processed the LiDAR data. S.H. conducted the statistical analyses and led the writing process. All authors contributed to the development of the study, interpretation of results and writing of the manuscript.

DATA ACCESSIBILITY

Data and R code are available on request.

ORCID

Samuel Hoffmann http://orcid.org/0000-0002-6176-8406
Alessandro Chiarucci https://orcid.org/0000-0003-1160-235X
Severin D.H. Irl http://orcid.org/0000-0002-1734-8607
Duccio Rocchini http://orcid.org/0000-0003-0087-0594
Ole R. Vetaas http://orcid.org/0000-0002-0185-1128
Mihai A. Tanase http://orcid.org/0000-0002-0045-2299
Stéphane Mermoz http://orcid.org/0000-0002-3166-7583
Alexandre Bouvet http://orcid.org/0000-0002-7428-4339
Carl Beierkuhnlein http://orcid.org/0000-0002-6456-4628

REFERENCES

Anderson, M. J. (2001). A new method for non-parametric multivariate analysis of variance. *Austral Ecology*, *26*, 32–46. https://doi.org/10.1111/j.1442-9993.2001.01070. pp. x

Anderson, M. J., Crist, T. O., Chase, J. M., Vellend, M., Inouye, B. D., Freestone, A. L., … Swenson, N. G. (2011). Navigating the multiple meanings of ß diversity: A roadmap for the practicing ecologist. *Ecology Letters*, *14*, 19–28. https://doi.org/10.1111/j.1461-0248.2010.01552.x

Arévalo, J. R., Fernández-Palacios, J. M., Jiménez, M. J., & Gil, P. (2001). The effect of fire intensity on the understorey species composition of two *Pinus canariensis* reforested stands in Tenerife (Canary Islands). *Forest Ecology and Management*, *148*, 21–29. https://doi.org/10.1016/S0378-1127(00)00478-3

Auerbach, M., & Shmida, A. (1993). Vegetation change along an altitudinal gradient on Mt-Hermon, Israel – No evidence for discrete communities. *Journal of Ecology*, *81*, 25–33. https://doi.org/10.2307/2261221

Baillarin, S. J., Meygret, A., Dechoz, C., Petrucci, B., Lacherade, S., Tremas, T., … Spoto, F. (2012). *SENTINEL-2 level 1 products and image processing performances*. Geoscience and Remote Sensing Symposium (IGARSS), ISPRS Journal, IX-B1, 197-202. https://doi.org/10.1109/igarss.2012.6351959

Cardinale, B. J., Duffy, J. E., Gonzalez, A., Hooper, D. U., Perrings, C., Venail, P., … Kinzig, A. P. (2012). Biodiversity loss and its impact on humanity. *Nature*, *486*, 59. https://doi.org/10.1038/nature11148

Carracedo, J. C., Badiola, E. R., Guillou, H., De La Nuez, J., & Pérez Torrado, F. J. (2001). Geology and volcanology of La Palma and El Hierro, Western Canaries. *Estudios Geológicos*, *57*, 175–273.

Chiarucci, A. (2007). To sample or not to sample? That is the question.. for the vegetation scientist. *Folia Geobotanica*, *42*, 209–216. https://doi.org/10.1007/BF02893887

Chytrý, M., & Otýpková, Z. (2003). Plot sizes used for phytosociological sampling of European vegetation. *Journal of Vegetation Science*, *14*, 563–570. https://doi.org/10.1111/j.1654-1103.2003.tb02183.x

Clements, F. E. (1905). Scientific books: Research methods in ecology. *Science*, *22*, 45–46. https://doi.org/10.1126/science.22.550.45

Clements, F. E. (1916). *Plant succession: An analysis of the development of vegetation*. Washington, DC, USA: Carnegie Institute, Publication 242. https://doi.org/10.5962/bhl.title.56234

Climent, J., Tapias, R., Pardos, J. A., & Gil, L. (2004). Fire adaptations in the Canary Islands pine (*Pinus canariensis*). *Plant Ecology*, *171*, 185–196. https://doi.org/10.1023/B:VEGE.0000029374.64778.68

Cubas, J., Martín-Esquivel, J. L., Nogales, M., Irl, S. D. H., Hernández-Hernández, R., López-Darias, M., … González-Mancebo, J. M. (2018). Contrasting effects of invasive rabbits on endemic plants driving vegetation change in a subtropical alpine insular environment. *Biological Invasions*, *20*, 793–807. https://doi.org/10.1007/s10530-017-1576-0

Del Arco Aguilar, M. J., González-González, R., Garzón-Machado, V., & Pizarro-Hernández, B. (2010). Actual and potential natural vegetation on the Canary Islands and its conservation status. *Biodiversity and Conservation*, *19*, 3089–3140. https://doi.org/10.1007/s10531-010-9881-2

Druitt, D. G., Enright, N. J., & Ogden, J. (1990). Altitudinal zonation in the mountain forests of Mt. Hauhungatahi, North Island, New Zealand. *Journal of Biogeography*, *17*, 205–220. https://doi.org/10.2307/2845327

Enright, N. (1982). The ecology of *Araucaria* species in New Guinea. I. Ordination studies of forest types and environments. *Austral Ecology*, *7*, 23–38. https://doi.org/10.1111/j.1442-9993.1982.tb01297.x

European Space Agency (2017). *Copernicus sentinel data*. Retrieved from https://scihub.copernicus.eu/dhus/#/home

Frampton, W. J., Dash, J., Watmough, G., & Milton, E. J. (2013). Evaluating the capabilities of Sentinel-2 for quantitative estimation of biophysical variables in vegetation. *ISPRS Journal of Photogrammetry and Remote Sensing*, *82*, 83–92. https://doi.org/10.1016/j.isprsjprs.2013.04.007

Gamon, J., Serrano, L., & Surfus, J. S. (1997). The photochemical reflectance index: An optical indicator of photosynthetic radiation

use efficiency across species, functional types, and nutrient levels. *Oecologia*, *112*, 492–501. https://doi.org/10.1007/s004420050337

Garzón-Machado, V., Otto, R., & del Arco Aguilar, M. J. (2013). Bioclimatic and vegetation mapping of a topographically complex oceanic island applying different interpolation techniques. *International Journal of Biometeorology*, *58*, 887–899. https://doi.org/10.1007/s00484-013-0670-y

Gitelson, A. A., Merzlyak, M. N., & Chivkunova, O. B. (2001). Optical properties and nondestructive estimation of anthocyanin content in plant leaves. *Photochemistry and Photobiology*, *74*, 38–45. https://doi.org/10.1562/0031-8655(2001) 0740038OPANEO2.0.CO2

Gitelson, A. A., Zur, Y., Chivkunova, O. B., & Merzlyak, M. N. (2002). Assessing Carotenoid Content in Plant Leaves with Reflectance Spectroscopy. *Photochemistry and Photobiology*, *75*, 272–281. https://doi.org/10.1562/0031-8655(2002) 0750272ACCIPL2.0.CO2

González Henríquez, M. N., Rodrigo Pérez, J. D., & Suárez Rodríguez, C. (1986). *Flora y Vegetacio ′n del Archipelago Canario*. Las Palmas de Gran Canaria, Spain: Edrica.

Hall, K., Reitalu, T., Sykes, M. T., & Prentice, H. C. (2012). Spectral heterogeneity of QuickBird satellite data is related to fine-scale plant species spatial turnover in semi-natural grasslands. *Applied Vegetation Science*, *15*, 145–157. https://doi.org/10.1111/j.1654-109X.2011.01143.x

Hamilton, A. C. (1975). A quantitative analysis of altitudinal zonation in Uganda forests. *Vegetatio*, *30*, 99–106. https://doi.org/10.1007/BF02389611

Hamilton, A. C., & Perrott, R. A. (1981). A study of altitudinal zonation in the montane forest belt of Mt. Elgon, Kenya/Uganda. *Vegetatio*, *45*, 107–125. https://doi.org/10.1007/BF00119220

He, K. S., & Zhang, J. (2009). Testing the correlation between beta diversity and differences in productivity among global ecoregions, biomes, and biogeographical realms. *Ecological Informatics*, *4*, 93–98. https://doi.org/10.1016/j.ecoinf.2009.01.003

He, K. S., Zhang, J., & Zhang, Q. (2009). Linking variability in species composition and MODIS NDVI based on beta diversity measurements. *Acta Oecologica*, *35*, 14–21. https://doi.org/10.1016/j.actao.2008.07.006

Höllermann, P. (2000). The impact of fire in Canarian ecosystems 1983–1998. *Erdkunde*, *54*, 70–75. https://doi.org/10.3112/erdkunde

Horning, N., Robinson, J. A., Sterling, E. J., Turner, W., & Spector, S. (2010). *Remote sensing for ecology and conservation. A handbook of techniques*. Oxford, UK: Oxford University Press.

Hufkens, K., Scheunders, P., & Ceulemans, R. (2009). Ecotones in vegetation ecology: Methodologies and definitions revisited. *Ecological Research*, *24*, 977–986. https://doi.org/10.1007/s11284-009-0584-7

Hunt, E., & Rock, B. (1989). Detection of changes in leaf water content using near- and middle-infrared reflectances. *Remote Sensing of Environment*, *30*, 43–54. https://doi.org/10.1016/0034-4257(89)90046-1

Irl, S. D. H., Harter, D. E. V., Steinbauer, M. J., Gallego Puyol, D., Fernández-Palacios, J. M., Jentsch, A., & Beierkuhnlein, C. (2015). Climate vs. topography – spatial patterns of plant species diversity and endemism on a high-elevation island. *Journal of Ecology*, *103*, 1621–1633. https://doi.org/10.1111/1365-2745.12463

Irl, S. D. H., Steinbauer, M. J., Babel, W., Beierkuhnlein, C., Blume-Werry, G., Messinger, J., … Jentsch, A. (2012). An 11-yr exclosure experiment in a high-elevation island ecosystem: Introduced herbivore impact on shrub species richness, seedling recruitment and population dynamics. *Journal of Vegetation Science*, *23*, 1114–1125. https://doi.org/10.1111/j.1654-1103.2012.01425.x

Irl, S. D. H., Steinbauer, M. J., Messinger, J., Blume-Werry, G., Palomares-Martínez, Á., Beierkuhnlein, C., & Jentsch, A. (2014). Burned and devoured – introduced herbivores, fire, and the endemic flora of the high-elevation ecosystem on La Palma, Canary Islands. *Arctic, Antarctic, and Alpine Research*, *46*, 859–869. https://doi.org/10.1657/1938-4246-46.4.859

Jax, K. (2006). Ecological units: Definitions and application. *The Quarterly Review of Biology*, *81*, 237–258. https://doi.org/10.1086/506237

Karger, D. N., Kluge, J., Krömer, T., Hemp, A., Lehnert, M., & Kessler, M. (2011). The effect of area on local and regional elevational patterns of species richness. *Journal of Biogeography*, *38*, 1177–1185. https://doi.org/10.1111/j.1365-2699.2010.02468.x

Lawton, J. H. (1999). Are there general laws in ecology? *Oikos*, *84*, 177–192. https://doi.org/10.2307/3546712

Legendre, P., & Anderson, M. J. (1999). Distance-based redundancy analysis: Testing multispecies responses in multifactorial ecological experiments. *Ecological Monographs*, *69*, 1–24. https://doi.org/10.1890/0012-9615(1999) 069[0001:DBRATM]2.0.CO;2

Legendre, P., & De Cáceres, M. (2013). Beta diversity as the variance of community data: Dissimilarity coefficients and partitioning. *Ecology Letters*, *16*, 951–963. https://doi.org/10.1111/ele.12141

Livingston, B. E. (1903). The distribution of the upland plant societies of Kent County, Michigan. *Botanical Gazette*, *35*, 36–55. https://doi.org/10.1086/328315

Lloyd, S. P. (1982). Least squares quantization in PCM. Technical Note, Bell Laboratories. *IEEE Transactions on Information Theory*, *28*, 128–137. https://doi.org/10.1109/TIT.1982.1056489

Lloyd, K., McQueen, A., & Lee, B. (2000). Evidence on ecotone concepts from switch, environmental and anthropogenic ecotones. *Journal of Vegetation Science*, *11*, 903–910. https://doi.org/10.2307/3236560

Mantel, N. (1967). The detection of disease clustering and a generalized regression approach. *Cancer Research*, *27*, 209–220.

Mardia, K. V., Kent, J. T. & Bibby, J. M. (1979). *Multivariate analysis*. London: Academic Press.

McCune, B., & Grace, J. B. (2002). *Analysis of ecological communities*. Gleneden Beach, OR, USA: MjM Software Design.

Méndez, J., Morales, G., de Nascimento, L., Otto, R., Gallardo, A., & Fernández-Palacios, J. M. (2015). Understanding long-term post-fire regeneration of a fire-resistant pine species. *Annals of Forest Science*, *72*, 609–619. https://doi.org/10.1007/s13595-015-0482-9

Merzlyak, M. N., Gitelson, A. A., Chivkunova, O. B., & Rakitin, V. Y. (1999). Non-destructive optical detection of pigment changes during leaf senescence and fruit ripening. *Physiologia Plantarum*, *106*, 135–141. https://doi.org/10.1034/j.1399-3054.1999.106119.x

Molina-Terrén, D. M., Fry, D. L., Grillo, F. F., Cardil, A., & Stephens, S. L. (2016). Fire history and management of *Pinus canariensis* forests on the western Canary Islands Archipelago, Spain. *Forest Ecology and Management*, *382*, 184–192. https://doi.org/10.1016/j.foreco.2016.10.007

Muer, T., Sauerbier, H., & Calixto, C. (2016). *Die Farn- und Blütenpflanzen der Kanarischen Inseln*. Weikersheim, Germany: Margraf.

Nagendra, H., & Rocchini, D. (2008). High resolution satellite imagery for tropical biodiversity studies: The devil is in the detail. *Biodiversity and Conservation*, *17*, 3431–3442. https://doi.org/10.1007/s10531-008-9479-0

Nagendra, H., Rocchini, D., Ghate, R., Sharma, B., & Pareeth, S. (2010). Assessing plant diversity in a dry tropical forest: Comparing the utility of Landsat and IKONOS satellite images. *Remote Sensing*, *2*, 478–496. https://doi.org/10.3390/rs2020478

Ogden, J., & Powell, J. (1979). A quantitative description of the forest vegetation on an altitudinal gradient in the Mount Field National Park, Tasmania, and a discussion of its history and dynamics. *Austral Ecology*, *4*, 293–325. https://doi.org/10.1111/j.1442-9993.1979.tb01220.x

Ørka, H. O., Wulder, M. A., Gobakken, T., & Næsset, E. (2012). Subalpine zone delineation using LiDAR and Landsat imagery. *Remote Sensing of Environment*, *119*, 11–20. https://doi.org/10.1016/j.rse.2011.11.023

Otto, R., García-del-Rey, E., Méndez, J., & Fernández-Palacios, J. M. (2012). Effects of thinning on seed rain, regeneration and understory vegetation in a *Pinus canariensis* plantation (Tenerife, Canary Islands). *Forest Ecology and Management*, *280*, 71–81. https://doi.org/10.1016/j.foreco.2012.05.027

Palmer, M. W., Earls, P. G., Hoagland, B. W., White, P. S., & Wohlgemuth, T. (2002). Quantitative tools for perfecting species lists. *Environmetrics*, *13*, 121–137. https://doi.org/10.1002/env.516

Palmer, M. W., & White, P. S. (1994). On the existence of ecological communities. *Journal of Vegetation Science*, *5*, 279–282. https://doi.org/10.2307/3236162

Palomares Martínez, Á., López Graciano, C., Freixes Montes, F., Gómez Gómez, M., Moral del Barrio, M. F., León Pérez, A. M., … Fernandez San Martín, J. M. (2011). *Memoria anual del Parque Nacional de La Caldera de Taburiente de 2012*. Madrid, Spain: Sapin, Ministerio de Medio Ambiente, y Medio Rural, y Marino.

Pettorelli, N. (2013). *The normalized difference vegetation index*. Oxford, UK: Oxford University Press. https://doi.org/10.1093/acprof:osobl/9780199693160.001.0001

Pettorelli, N., Laurance, W. F., O'Brien, T. G., Wegmann, M., Nagendra, H., & Turner, W. (2014). Satellite remote sensing for applied ecologists: Opportunities and challenges. *Journal of Applied Ecology*, *51*, 839–848. https://doi.org/10.1111/1365-2664.12261

Rees, W. G. (2007). Characterisation of Arctic treelines by LiDAR and multispectral imagery. *Polar Record*, *43*, 345–352. https://doi.org/10.1017/S0032247407006511

Ricklefs, R. (1987). Community diversity: Relative roles of local and regional processes. *Science*, *235*, 167–171. https://doi.org/10.1126/science.235.4785.167

Ricklefs, R. E. (2008). Disintegration of the ecological community. American society of naturalists Sewall Wright award winner address. *The American Naturalist*, *172*, 741–750. https://doi.org/10.1086/593002

Rocchini, D. (2007). Effects of spatial and spectral resolution in estimating ecosystem α-diversity by satellite imagery. *Remote Sensing of Environment*, *111*, 423–434. https://doi.org/10.1016/j.rse.2007.03.018

Rocchini, D., Balkenhol, N., Carter, G. A., Foody, G. M., Gillespie, T. W., He, K. S., … Nagendra, H. (2010). Remotely sensed spectral heterogeneity as a proxy of species diversity: Recent advances and open challenges. *Ecological Informatics*, *5*, 318–329. https://doi.org/10.1016/j.ecoinf.2010.06.001

Rocchini, D., Boyd, D. S., Féret, J. B., Foody, G. M., He, K. S., Lausch, A., … Pettorelli, N. (2016). Satellite remote sensing to monitor species diversity: Potential and pitfalls. *Remote Sensing in Ecology and Conservation*, *2*, 25–36. https://doi.org/10.1002/rse2.9

Rocchini, D., Butini, S. A., & Chiarucci, A. (2005). Maximizing plant species inventory efficiency by means of remotely sensed spectral distances. *Global Ecology and Biogeography*, *14*, 431–437. https://doi.org/10.1111/j.1466-822x.2005.00169.x

Rocchini, D., Chiarucci, A., & Loiselle, S. A. (2004). Testing the spectral variation hypothesis by using satellite multispectral images. *Acta Oecologica*, *26*, 117–120. https://doi.org/10.1016/j.actao.2004.03.008

Schmidtlein, S., & Fassnacht, F. E. (2017). The spectral variability hypothesis does not hold across landscapes. *Remote Sensing of Environment*, *192*, 114–125. https://doi.org/10.1016/j.rse.2017.01.036

Sha, Z., Bai, Y., Xie, Y., Yu, M., & Zhang, L. (2008). Using a hybrid fuzzy classifier (HFC) to map typical grassland vegetation in Xilin River Basin, Inner Mongolia, China. *International Journal of Remote Sensing*, *29*, 2317–2337. https://doi.org/10.1080/01431160701408436

Shipley, B., & Keddy, P. A. (1987). The individualistic and community-unit concepts as falsifiable hypotheses. *Vegetatio*, *69*, 47–55. https://doi.org/10.1007/BF00038686

Siegel, S., & Castellan, N. J. (1988). *Non-parametric statistics for the behavioural sciences*. New York, NY, USA: MacGraw Hill.

Simpson, E. (1949). Measurement of diversity. *Nature*, *163*, 688. https://doi.org/10.1038/163688a0

Sims, D. A., & Gamon, J. A. (2002). Relationships between leaf pigment content and spectral reflectance across a wide range of species, leaf structures and developmental stages. *Remote Sensing of Environment*, *81*, 337–354. https://doi.org/10.1016/S0034-4257(02)00010-X

Socolar, J. B., Gilroy, J. J., Kunin, W. E., & Edwards, D. P. (2016). How should beta-diversity inform biodiversity conservation? *Trends in Ecology & Evolution*, *31*, 67–80. https://doi.org/10.1016/j.tree.2015.11.005

Strayer, D. L., Power, M. E., Fagan, W. F., Pickett, S. T. A., & Belnap, J. (2003). A classification of ecological boundaries. *BioScience*, *53*, 723–729. https://doi.org/10.1641/0006-3568(2003) 053[0723:ACOEB]2.0.CO;2

Vellend, M. (2010). Conceptual synthesis in community ecology. *The Quarterly Review of Biology*, *85*, 183–206. https://doi.org/10.1086/652373

Vellend, M., Verheyen, K., Flinn, K. M., Jacquemyn, H., Kolb, A., Van Calster, H., … Hermy, M. (2007). Homogenization of forest plant communities and weakening of species–environment relationships via agricultural land use. *Journal of Ecology*, *95*, 565–573. https://doi.org/10.1111/j.1365-2745.2007.01233.x

Walker, D., & Guppy, J. (1976). Generic plant assemblages in the highland forests of Papua New Guinea. *Austral Ecology*, *1*, 203–212. https://doi.org/10.1111/j.1442-9993.1976.tb01109.x

Walker, S., Wilson, J. B., Steel, J. B., Rapson, G. L., Smith, B., King, W. M., & Cottam, Y. H. (2003). Properties of ecotones: Evidence from five ecotones objectively determined from a coastal vegetation gradient. *Journal of Vegetation Science*, *14*, 579–590. https://doi.org/10.1111/j.1654-1103.2003.tb02185.x

Whittaker, R. H. (1956). Vegetation of the great smoky mountains. *Ecological Monographs*, *26*, 1–80. https://doi.org/10.2307/1943577

Whittaker, R. H. (1967). Gradient analysis of vegetation. *Biological Reviews of the Cambridge Philosophical Society*, *42*, 207–264. https://doi.org/10.1111/j.1469-185X.1967.tb01419.x

Whittaker, R. H. (1970). *Communities and ecosystems*. London, UK: MacMillan.

Wiens, J. A., Crawford, C. S., Gosz, J. R., Crawford, S., & Boundary, J. R. (1985). Boundary dynamics: A conceptual framework for studying landscape ecosystems. *Oikos*, *45*, 421–427. https://doi.org/10.2307/3565577

Wilson, J. B., & Agnew, A. D. Q. (1992). Positive-feedback switches in plant communities. *Advances in Ecological Research*, *23*, 263–336. https://doi.org/10.1016/S0065-2504(08)60149-X

Wood, S. N. (2017). *Generalized additive models: An introduction with R*. Boca Raton, FL, USA: Chapman & Hall/CRC Press.

Xie, Y., Sha, Z., & Yu, M. (2008). Remote sensing imagery in vegetation mapping: A review. *Journal of Plant Ecology*, *1*, 9–23. https://doi.org/10.1093/jpe/rtm005

SUPPORTING INFORMATION

Additional supporting information may be found online in the Supporting Information section at the end of the article.

Appendix S1. Supporting tables and figures.

Appendix S2. LiDAR product description.

How to cite this article: Hoffmann S, Schmitt TM, Chiarucci A, et al. Remote sensing of β-diversity: Evidence from plant communities in a semi-natural system. *Appl Veg Sci*. 2019;22:13–26. https://doi.org/10.1111/avsc.12403